

Full Length Research Paper

Preparation, characterization and *in vitro* study of biocompatible fibroin hydrogel

M. K. Sah and K. Pramanik*

Department of Biotechnology and Medical Engineering, National Institute of Technology, Rourkela, Orissa-769008, India.

Accepted 26 April, 2011

In this study, *Bombyx mori* silk based hydrogels were prepared and their biorelevant properties like physical, chemical and thermal properties were studied. Firstly, silk fibroin aqueous solution was prepared and the molecular weight of fibroin protein was determined followed by particle size analysis for the confirmation of study. Silk fibroin hydrogels were prepared by treating a 12% (w/v) silk fibroin aqueous solution at 4°C (thermgel) and lyophilized. The swelling and thermorheological behaviour of fibroin hydrogels were studied. The morphology and crystalline structure of lyophilized hydrogels were investigated by scanning electron microscopy (SEM) and wide-angle diffractometry, respectively while the surface functional groups were analyzed by FT-IR. The thermal behavior was also studied by means of differential scanning calorimetry and gravimetric method. The cytocompatibility of the hydrogels was evaluated through three-dimensional culture with human peripheral blood mononuclear cells. Lyophilized fibroin gel of high strength and high thermal stability were obtained. The β -crystalline structure of lyophilized fibroin hydrogel has shown excellent swelling capacity to mimic the living tissues. The surfaces of these hydrogels were found supporting to cell adherence and proliferation. hMNCs could survive and proliferate in the gel within 3 weeks, and the gel had good cytocompatibility. It was concluded that fibroin hydrogel not only has interpenetrating network structure but also has good cytocompatibility and could be used as injectable scaffolds able to promote *in situ* bone regeneration.

Key words: Fibroin, hydrogel, tissue engineering, sodium dodecyl sulfate polyacrylamide gel electrophoresis, scanning electron microscopy, cytocompatibility.

INTRODUCTION

Millions of people every year worldwide suffer from injured and deficient tissues or damaged organ. In such cases, only two therapeutic choices such as mechanical replacement and organ transplantation are employed. However, these approaches encounter several clinical issues such as poor biocompatibility of biomaterials used for making artificial organs, shortage of organ donors or the adverse effects of immunosuppressive agents. To break through the problems regenerative medical therapy has been considered as promising strategy to cure the disease based on the natural healing potential of patients. One such technique is tissue engineering, which has been evolved as more advanced and promising

approach to regenerate tissues and organs. One of the major aspects of this technique is the development of scaffold from biocompatible and biodegradable polymers (Peppas, 1997). Hydrogels are three-dimensional polymeric networks prepared by physical or chemical cross linking and resistant to swelling in aqueous solution without dissolving in it (Vepari and Kaplan, 2007; Lee and Mooney; 2001). Since hydrogels are highly hydrated hydrophilic polymer networks that contain pores and void spaces between the polymer chains, it can be implanted for tissue restoration or local release of therapeutic factors. Such hydrogels provide many advantages over the common conventional solid scaffold materials, including an enhanced supply of nutrients and oxygen for the cells. Pores within the network provide space to cells for proliferation and expansion. Due to their high water content hydrogels thus, are similar to some tissues and

*Corresponding author. E-mail: kpr@nitrrkl.ac.in.

extracellular matrices (ECM) (Park and Lakes, 1992).

Widespread research is under way on using hydrogels as scaffold materials for application in tissue engineering, where the spaces might be filled with stem cells, growth factors or both. Hydrogels prepared from variety of polymers such as alginates, chitosan and collagen have been extensively studied for use as scaffold in tissue engineering (Lee et al., 2001; Drury and Mooney, 2003). Hydrogels formed from synthetic polymers offer the benefit of gelation and gel properties that are controllable and reproducible through the use of specific molecular weights, block structures, and modes of cross linking but the less biocompatibility and use of toxic reagents limits their application. Generally, gelation of naturally derived polymers is reported to be less controllable; although, the hydrogels formed are more compatible for hosting cell and bioactive molecules (Lee and Mooney, 2001; Smidsrod and Skjaok, 1990). Injectable biomaterials for tissue engineering are defined as cell seeded engineered scaffolds directly injected at the site of the site of defect. Such fluidly material takes the complex shape of site, fixes it and exchanged with body fluid. Seeded cell proliferate and differentiate to form tissues. Such approach in tissue engineering reduces the surgical operations (Balakrishnan and Jayakrishnan, 2005; Kretlow et al., 2007). *Bombyx mori* silk, a member of Bombycidae family is composed of a filament core fibroin proteins cemented together with glue-like sericine proteins (Kaplan et al., 1994; Magoshi et al., 1996). Silk due to its unique combination of properties such as mechanical strength, biodegradability and biocompatibility is considered as a potential matrix for controlled release in various forms which include fibroin scaffolds, electrospun woven mats, silk microspheres and silk fibroin films (Altman et al., 2003; Uebersax et al., 2008; Li et al., 2006; Wang et al., 2007; Hofmann et al., 2006).

Silk fibroin hydrogels are of great interest for drug delivery and tissue engineering applications. Recently, many applications suggest the potential of porous hydrogels for cell culture and regenerative medicine (Hanawa et al., 1995; Fini et al., 2005). Fini et al. (2005) found that low pH induced silk fibroin hydrogels shows better healing of cancellous rabbit distal femurs than the control material, poly (D, L lactide-glycolide) as a bone-filling biomaterial (Fini et al., 2005). For many cell-based applications, gelation must be induced under mild conditions to reserve its mechanical and biocompatibility properties which could potentially alter cell function and affect cell viability. The study of Silk Fibroin (SF) hydrogels formation is important for understanding the behavior of SF metastable solution. During the gelation process, SF experiences transition in structure from random coil to β -sheet due to enhanced hydrophobic interactions and hydrogen bond formation leading to form a more stable structure (Hanawa et al., 1995; Kim et al., 2004; Motta et al., 2004; Ayub et al., 1994; Kang et al., 2000). The objective of the present paper was to examine

the processability of concentrated aqueous silk fibroin solutions into highly porous gel sponges and study of their various properties for possible tissue engineering applications.

MATERIALS AND METHODS

Preparation of aqueous silk fibroin solution

Domesticated *B. mori* silk cocoon used for this study were obtained from Mulberry Farms of chitoor district, Hyderabad (India). Dried cocoon shells were cut into small pieces and treated with boiling aqueous solution of sodium carbonate of varying concentration with stirring. The whole mass was repeatedly washed with Milli-Q water to remove the glue-like sericine protein and kept in hot air oven for drying. Silk fibroin solution was prepared by dissolving 10 g of degummed silk in 9.3 M LiBr solution at 70°C for 2½ h. The fibroin solution was dialyzed in a cellulose membrane based dialysis cassette (molecular cutoff 12,400) against deionized water for 3 days, changing water every 6 h in order to completely remove LiBr. After dialysis, silk fibroin solution was centrifuged at 5 to 10°C and 9000 rpm for 20 min to remove impurities and precipitated matter. The concentration of the silk fibroin aqueous solution at the end was 12 wt%.

Preparation of silk fibroin hydrogels and sponges

The regenerated silk fibroin prepared as earlier, when kept at 20°C for 3 days under humid environment to form translucent silk fibroin hydrogels (thermgels). The hydrogels such obtained when kept at -20°C for 24 h and lyophilized for the next 24 h formed fibroin sponges.

Swelling property of silk hydrogel

The swelling properties of the hydrogels were studied using conventional gravimetric method (Vazquez et al., 1997). The swelling behavior of dried hydrogels was monitored as a function and was determined by immersing the completely dried (60°C for 24 h) hydrogel samples in double-distilled water at 37°C. Swollen gels were weighed by an electronic balance at pre-determined time intervals after wiping excess surface liquid by filter paper. The swelling ratio (SR) was calculated from the following equation:

$$SR = \frac{M_t - M_o}{M_o}$$

Where, M_t is the mass of the swollen gel at time t and M_o is the mass of the dry gel at time 0.

Rheological properties

The rheological property of the prepared silk fibroin solution was assayed by measuring the viscosity by a cone and plate viscometer (BOHLIN VISCO-88, Malvern, U.K.). The cone angle is 5.4° and diameter is 30 mm. A gap of 0.15 mm was maintained between the cone and plate for all the measurements. The temperature was maintained using an external water circulator as 30, 35, 40, 45, 50 and ± 1 °C.

Scanning electron microscopy

The morphology of silk fibroin samples were determined by SEM at different magnification. Samples were air-dried overnight and affixed via carbon tape to the SEM sample holders and vacuum-coated with a 20 nm layer of platinum. Specimens were observed on a JEOL JSM -6480LV SEM and photographed at a voltage of 15 kV at room temperature.

Measurement of molecular weight

The molecular weight of the regenerated silk fibroin was determined by sodium dodecyl sulfate polyacrylamide gel electrophoresis (SDS-PAGE) according to the method described by Laemmli (1970) using 12% acrylamide gel and 5% condensing gel, which was stained with the easy stain Commassie blue kit (Invitrogen, Carlsbad, CA).

Particle size analysis

Average particle size of regenerated silk fibroin in solution was measured by Zetasizer Nano ZS (Malvern, U.K) particle analyzer at 30°C after discarding precipitated impurities of centrifuged fibroin solution at 9000 rpm for 10 min at 10°C. Particle size measurement was based on laser beam scattering technique. The optic unit contained a 4 mW He-Ne (633 nm) laser.

X-ray diffraction

An X-ray diffractometer XRD (Phillips PW-1830) with Ni-filtered Cu-K α radiation operating at 35 kV and 30mA was used to record the diffraction pattern of samples of the degummed silk fiber and silk fibroin scaffold. Crystallinity was determined by integration using KaleidaGraph (Synergy Software).

FT-IR spectroscopy

The degummed silk fiber and lyophilized fibroin hydrogels were analyzed by FTIR spectroscopy. Room-temperature FT-IR spectra were recorded on solid samples in KBr pellets by means of a Shimadzu FT-IR spectrometer (IRPrestige-21) with a resolution of 4 cm⁻¹. The spectra were smoothed with constant smooth factor for comparison.

Differential scanning calorimetry

The thermal behavior of degummed silk fiber and lyophilized fibroin hydrogels were determined by means of differential scanning calorimetry (DSC) using a Mettler Toledo DSC822e differential scanning calorimeter. The samples used weighed between 10 and 15 mg and were measured between the ranges of -20 to 300°C at a scanning rate of 20°C/min under nitrogen atmosphere.

Thermal gravimetric analysis

The thermal stability degummed silk fiber and lyophilized fibroin hydrogels were characterized using a DTG-6H (Simadzu). The amount of sample for each measurement was about 1 mg, and all of the measurements were carried out under a nitrogen atmosphere and heated up to 700°C at a heating rate of 10°C min⁻¹.

Isolation and culture of hMNCs in silk gels

Mononuclear cells MNCs were isolated from fresh peripheral blood of healthy, middle aged human using Ficoll-paque separation technique as described previously (Neagu, 2005). The hMNCs culture were expanded in growth media containing 90% DMEM-F12, 10% fetal bovine serum (FBS), 100 U/mL penicillin, 1000 U/mL streptomycin and 0.2% fungizone antimycotic. After passaging of the culture 3 times, the culture were trypsinized and resuspended in DMEM-F12 to obtain a cell density of 3 x 10⁷ cells/mL. Autoclaved (sterilized) 15 ml of silk fibroin solution (12% w/v) were supplemented with powder DMEM-F12 and NaHCO₃. For the induction of gelation, solutions were sonicated for 20 min, continuously or with break of 5 to 10 min in a laminar hood. After sonication, solution was kept for 5 to 10 min for cooling at room temperature. A volume of 50 μ L cell suspension was added and well mixed with fibroin solution to make the final concentration of 1 X 10⁵ cells/mL. The solution was put into 5 culture Petri dishes (Tarson, 32 mm) and incubated at 37°C and 5% CO₂. At the end of day 3 and 7, small plugs were punched out of the gels, washed 2 to 3 times with PBS, cut into two halves and incubated in Trypan blue for 15 min at 37°C. The cell morphologies and viability were monitored using phase contrast light microscope (Carl Zeiss, Axiovert 40 C) equipped with a cannon 3 CCD color video camera.

The morphology of cell-scaffold constructs were determined by SEM after keeping in 2.8% gluteraldehyde solution overnight.

RESULTS AND DISCUSSION

Morphology of degummed silk fiber

The morphology of degummed silk fibroin was investigated by SEM (Figure 1). The native undegummed silk fiber (Figure 1a) clearly shows the smooth and sticking look due to the presence of sericine. The Figure 1b shows incomplete degumming while at 0.02 M concentration the complete removal of sericine was found. Surface with more rough look besides the complete removal of sericine was found with further increase in concentration (Figure 1c).

Characterization of silk fibroin

During dissolution of degummed silk fiber in LiBr, the amide bonds of fibroin molecular chain might be cleaved to different extent resulting in easy solubilization in water. The water soluble silk fibroin is called regenerated silk fibroin and are easily denatured and gelled by various factors. Despite of temperature and pH, the stability of silk fibroin solution largely depends on its molecular mass range. The silk fibroin aqueous solutions were kept at 4°C and characterization is done within a month. Figure 2(a) shows a smear band of silk fibroin corresponding to molecular marker ranging between 200 to 30 kDa. AS the result reveals, the regenerated protein solution were composed of a mixture of polypeptides with several molecular weights. A broad dull band from 200 to 35 kDa and a clear sharp band at 25 kDa are obtained. The former band might be degradation products of heavy chain (350 kDa) obtained due to cleavage of amide

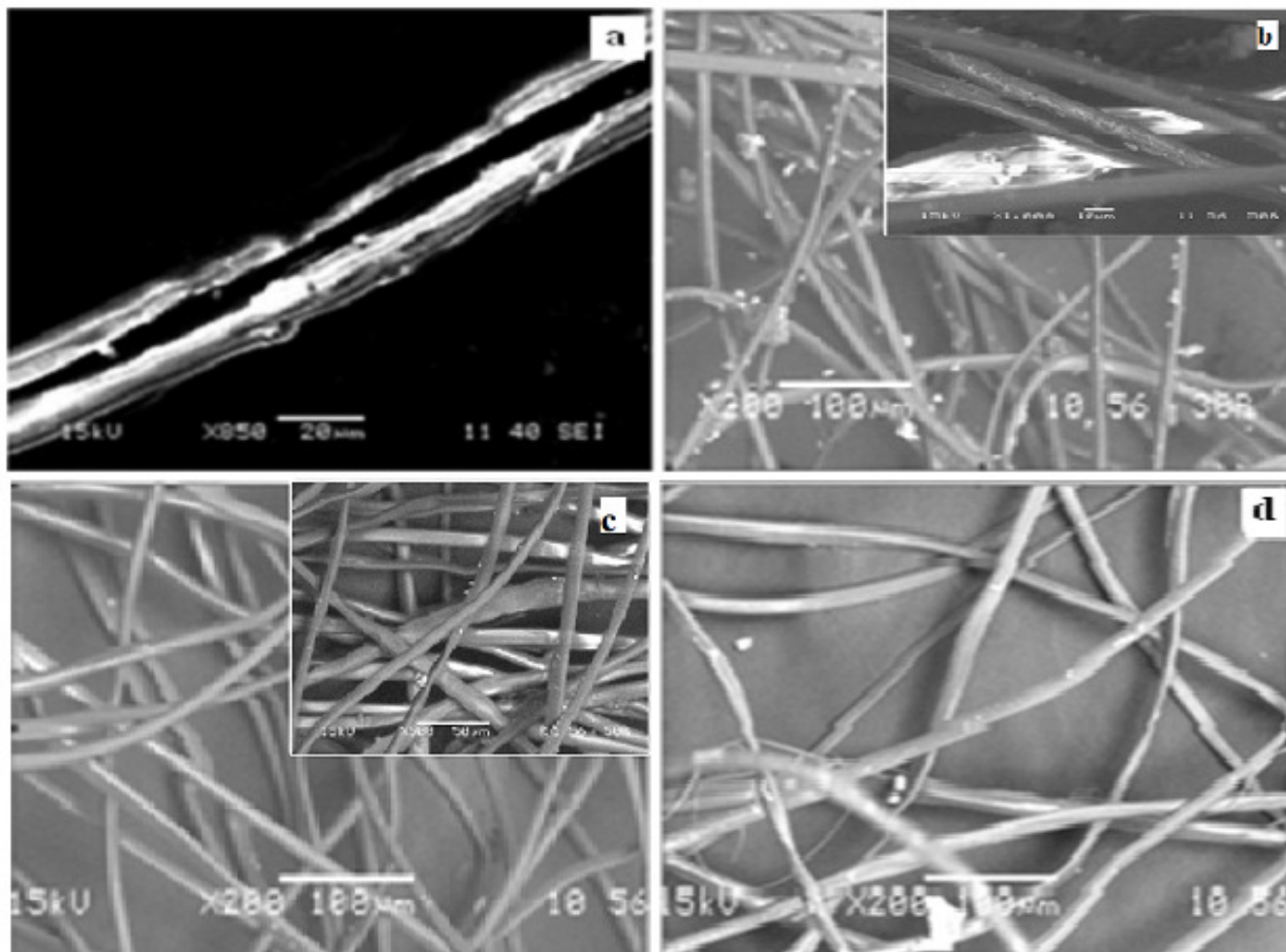


Figure 1. Scanning electron micrographs illustrating morphologies of fibroin silk prepared by degumming of silk cocoon. (a) Control silk. The sericin coating of two brins was clearly evident in control silk before degumming; (b) silk fibre degummed by 0.01 M Na_2CO_3 , showing comparatively incomplete removal of gum; (c) silk fibre degummed by 0.02 M Na_2CO_3 , appearing relatively smooth, and individual longitudinal strands were also clearly visible; (d) silk fibre degummed by 0.03 M Na_2CO_3 individual longitudinal strands were clearly visible.

bonds of raw silk protein formed by degumming and dissolution while, the band at 25 kDa corresponds to the light chain of raw silk protein. Result was confirmed by particle size analysis of silk fibroin solution. The results of size distribution (Figure 2b) were in good agreement with the results obtained from the molecular weight distributions.

As shown in Figure 2b, particle size distribution profile is bimodal, with peaks at around 100 nm and 5 μm . Since particle size of the starting SF solution is disintegrated due to processing of extraction using salts, the results confirm the presence of light chain (25 kDa) with disintegrated heavy chain (350 kDa) (Horan et al., 2005).

Morphological study of silk fibroin hydrogels

Morphologically, the hydrogels showed a sponge-like

cross-linked structure produced by physical entanglement as well as chemical hydrogen and covalent bindings. Water-stable hydrogels were formed from SF aqueous solutions after 24 h, which leads to the formation of porous matrices. This was due to induction of a sol-gel transition in the concentrated solution sample. Regenerated silk fibroin solution when kept at 20°C in humid environment for more than 72 h, the silk fibroin aqueous solution was converted into gel and the hydrogel (thermgel) is formed. The process was induced by adding few drops of methanol as crystallinity inducing solvent. The silk hydrogel intact in shape is formed and stabilized due to internetworking. The gel does not lose its integrity when kept vertically as shown in Figure 3(a). Figures 3(b, c and d) is a representative optical micrograph of prepared silk fibroin hydrogel sample as prepared. Morphological study of silk fibroin porous matrices was observed by SEM (Figures 4a and b) after lyophilizing the

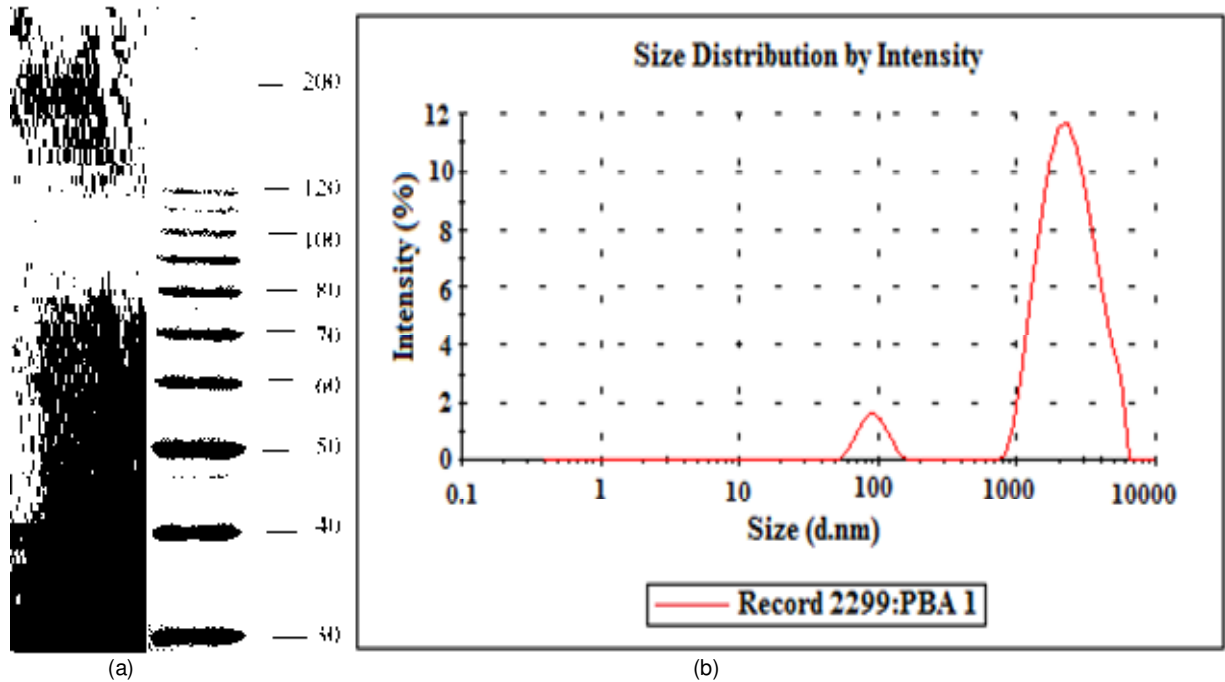


Figure 2. (a) SDS-PAGE (12% gel) of silk fibroin protein. Marker and fibroin lanes mean the standard protein ladder from 10 to 200 kDa (Gibco Co., USA) and the molecular mass range of silk fibroin, respectively; (b) particle size distribution of silk fibroin by particle analyzer.

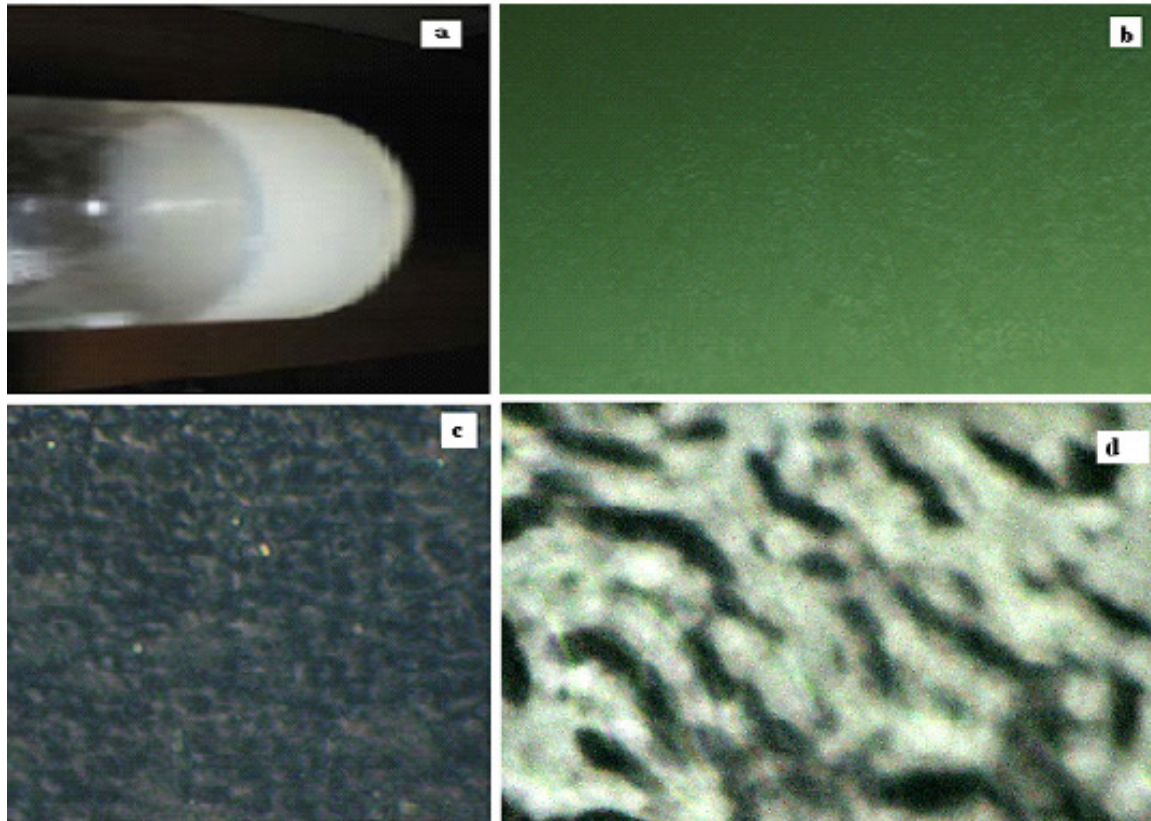


Figure 3. Silk fibroin hydrogel when kept at 20 °C for 3 days with conc. 12% (w/v) of silk fibroin. Simple eye view (a) and optical micrographs, 5X (b) 10X (c) and 20X (d).

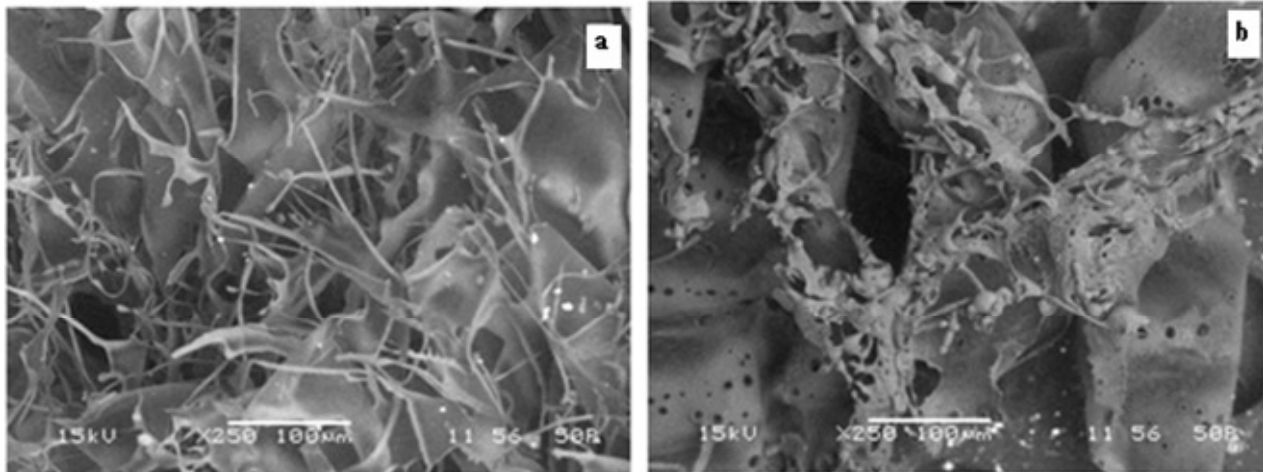


Figure 4. Scanning electron micrographs showing the porous lyophilized hydrogel leaf-like structure prepared from 4 wt% silk fibroin solution (a) and hydrogel sponge prepared from > 12 wt% silk fibroin solution (b).

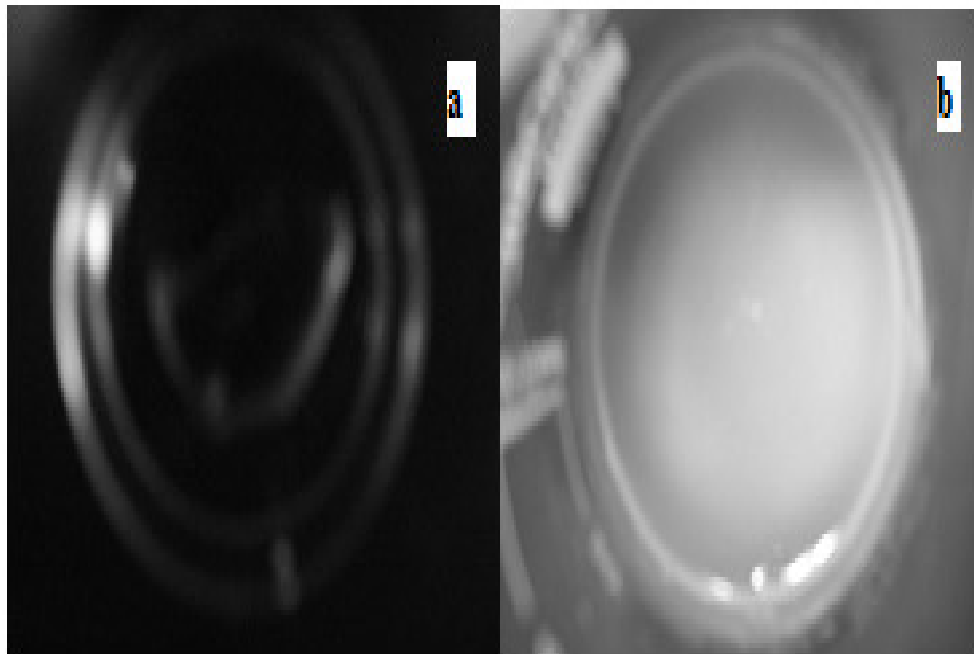


Figure 5. (a) Dehydrated gel and (b) swollen hydrogel (after 36 h kept in deionized water at 37°C).

hydrogel samples at -80°C . Lyophilized hydrogels prepared from silk fibroin solutions of 4 to 12 wt% concentration showed leaf-like morphologies while concentration more than 12 wt% exhibited sponge-like structures (Kim et al., 2004).

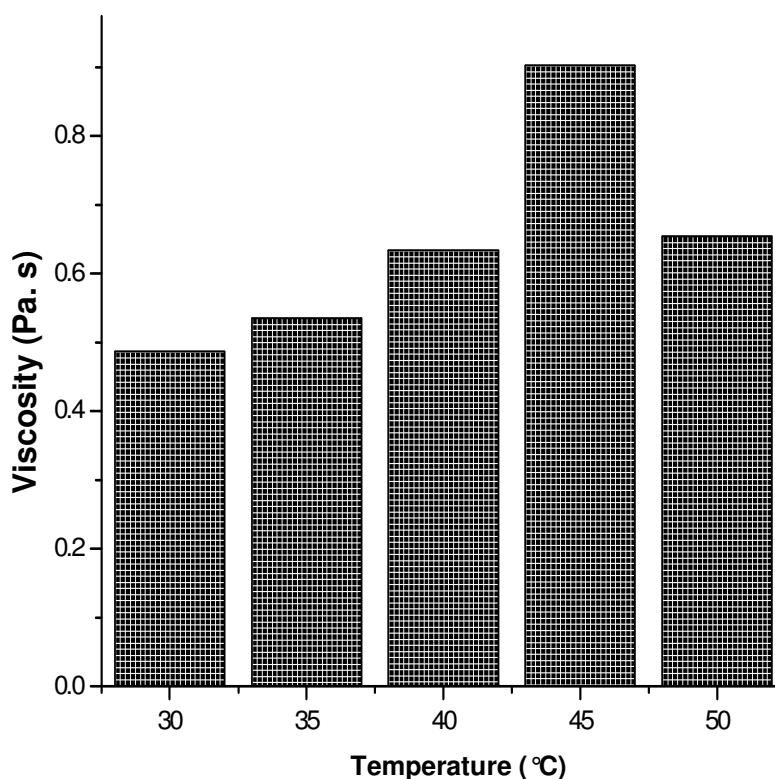
Swelling property of silk hydrogel

The swelling state of the polymer was reported to be

important for its bioadhesive property (Smart et al., 1984; Smart, 2005). It was found that the molecular structure of fibroin was not changed by the change in water content of the gel, while the physical properties of the gel, however, changes significantly (Ayub et al., 1993). It can be observed from Figure 5 that water uptake by hydrogels increased with time until they attained equilibrium. Table 1 shows the swelling behaviour of dehydrated hydrogel kept in deionized water at 37°C for different time intervals. The complete removal of water from hydrogel

Table 1. Gain in water content (w/w%) of dehydrated hydrogel kept in deionized water at different time (h) interval.

| Time (h) | Weight of gel (mg) | Swelling ratio (%) |
|----------|--------------------|--------------------|
| 0 | 77.19 | 0 |
| 2 | 135.12 | 75.05 |
| 4 | 244.14 | 216.28 |
| 16 | 298.54 | 286.76 |
| 24 | 301.12 | 290.1 |
| 28 | 301.15 | 290.14 |
| 32 | 301.155 | 290.15 |
| 36 | 301.155 | 290.15 |

**Figure 6.** Newtonian behavior showing the linear relation between shear stress and shear rate studied between the temperature range of 30 to 50 °C.

during dehydration was assumed when no further change in weight was found. The dehydrated gel was non-brittle showing presence of water molecule to maintain equilibrium with respect to physical properties of the gel. The brittle gel could be found when dehydrated in the oven. The swelling rate was higher during the initial stage indicating the sucking of water molecules into the collapsed gel and adsorption of water over the dried surface of gel. Within 2 h, the gel gains weight of 75.05 and 216.28% after 4 h indicating decline in swelling rate. After 24 h, the change was found to be 290.1% which was increased up to 290.15% at 32 h. No further change was observed after this period. After this period, the

water molecule goes inside the collapsed gel network at a much slower rate. The thermorheological behavior of the silk fibroin hydrogel prepared by incubating the fibroin solution at 20 °C for 7 days was examined with initial fibroin concentration of 12% (w/v) in the temperature range from 30 to 50 °C measuring “shear stress and viscosity” at 5 degrees interval. Figure 6 shows the changes in viscosity as temperature was increased. Recent DSC results of the silk fibroin samples reveals a broad endotherm with a peak near 45 °C indicating gradual structural change with increase in temperature and a new structure is formed above 45 °C. This thermal behavior shows consistency with the viscoelastic behavior.

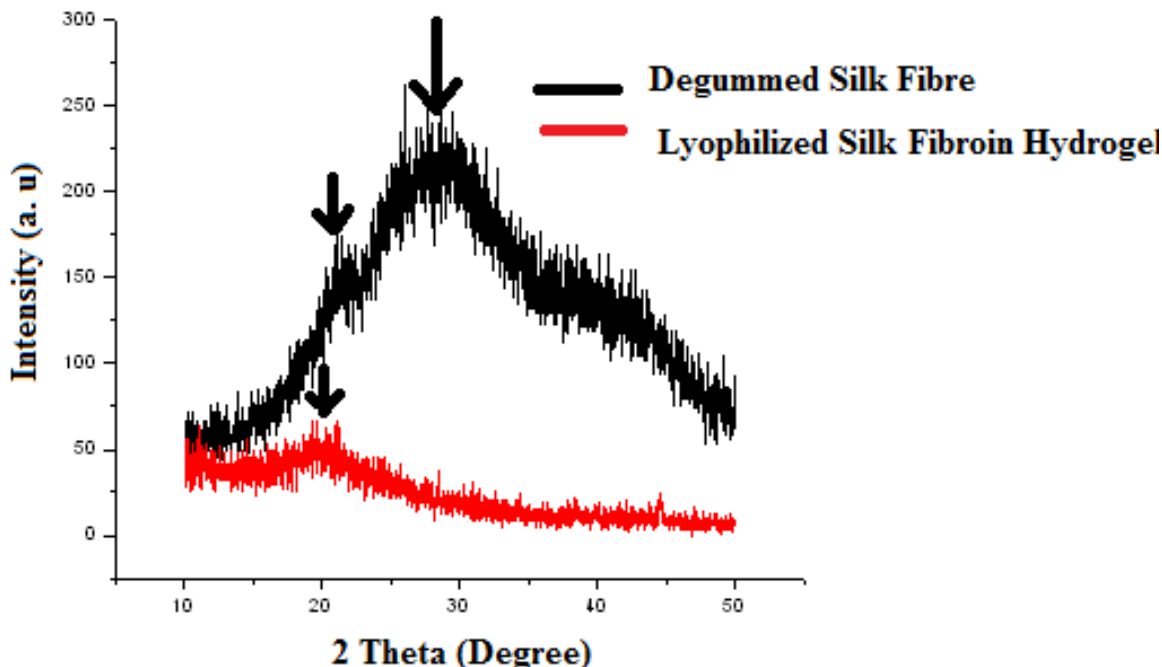


Figure 7. X-ray diffraction of (a) degummed silk fiber and (b) Lyophilized silk fibroin hydrogel.

Preliminary ATR FT-IR study has indicated that the fraction of antiparallel β -sheet conformation appreciably increased at 45°C (Ochi et al., 2002). Irreversible structural change could be considered as a reason to the thermoreheological behavior observed. The graphs plotted between viscosity and shear rate at different temperature showed the linearly proportionality at the low shear rate region of less than 100 s^{-1} . Rheopectic fluids increase their viscosity over time with application of shear forces, while thixotropic fluids have a reversible time-dependent loss of viscosity accompanying the application of shear force (Miller, 1960). If the time-dependent loss of viscosity is nonreversible, the fluid is considered to have rheodestructive properties. Study at different temperature shows, gel exhibits rheopectic properties and either thixotropic or rheodestructive properties. Repeated observation reveals that continuous swirling of the mixture leads to an irreversible decrease in the viscosity. Therefore, the time-dependent reduction in the gel's viscosity is rheodestructive rather than thixotropic.

Structural analysis

Structural characterization of silk fibroin fiber and lyophilized hydrogels were performed by X-ray diffraction and FTIR analysis. The XRD patterns and FTIR peaks of degummed silk fiber and lyophilized RSF hydrogel are shown in Figures 7 and 9 respectively. Figure 7 shows X-ray profiles of lyophilized hydrogels prepared from SF aqueous solutions. When silk fibroin solutions freeze at low temperature below the glass transition from -34 to -

20°C, the structure doesn't change significantly (Li et al., 2001). The amorphous structure of lyophilized silk fibroin hydrogel samples were indicated by exhibition of a broad peak at around 20° (Magoshi et al., 1996). Silk fibroin hydrogels showed a distinct peak at 20.6° and two minor peaks at around 9° and 24°, very similar to β -sheet crystalline silk fibroin structure (Silk I) (Ayub et al., 1993; Asakura et al., 1985). X-ray diffraction results showed that the gelation of silk fibroin solutions induced a transition from random coil to β -sheet conformation as reported previously (Hanawa et al., 1995; Ayub et al., 1993; Kang et al., 2000). The regenerated silk fibroin (RSF) hydrogel (line B in Figure 7) shows more amorphous state, while the degummed silk fiber (line A in Figure 8) shows a typical X-ray diffractogram of β -sheet crystalline structure, which has four diffraction peaks at 18.9°, 20.6°, 24.3° and 28.1°, corresponding to β -sheet crystalline spacing of 4.69°, 4.31°, 3.66°, 3.17 Å, respectively (Ayub et al., 1993; Asakura et al., 1985). While the lyophilized fibroin hydrogel shows the characteristic peak at 20.6° while other peaks corresponding to degummed silk fiber is not visible indicating the more α -helical secondary structure. In conclusion, the processing of silk fibroin results into loss of β -sheet structure thus liable to be more biodegradability and loss in mechanical strength.

The functional groups over the surface were analyzed by FT-IR for more detail. Since the IR spectrum represents typical absorption bands sensitive to the molecular conformation of SF, scientists' oftenly investigate the conformation of SF and its blend using IR spectroscopy. In order to confirm the conformational changes of SF,

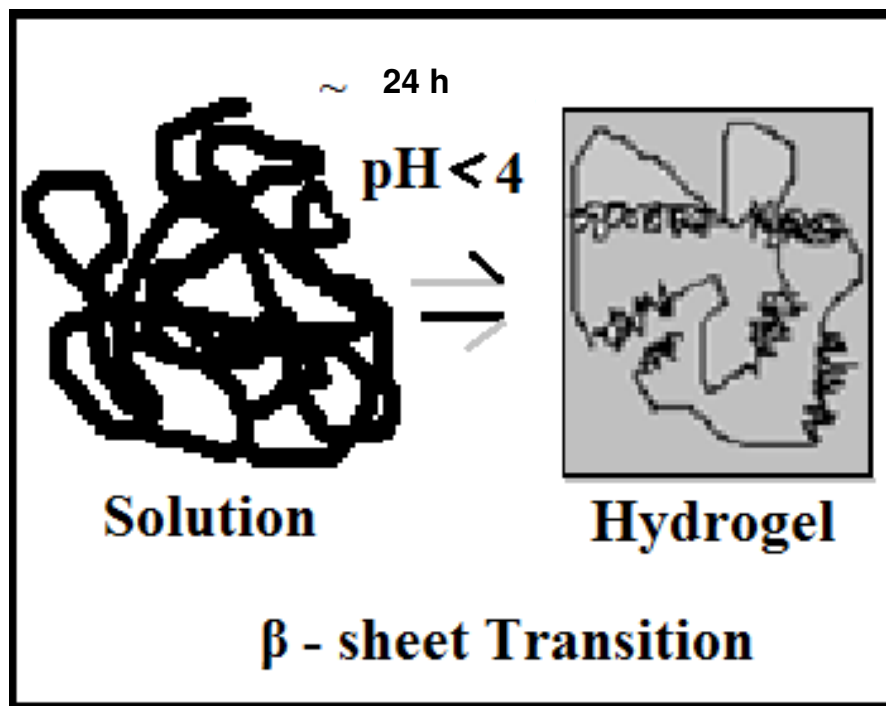


Figure 8. Sol-gel transition of silk fibroin.

FTIR spectroscopy was performed and the results for degummed silk fibroin and lyophilized silk fibroin hydrogel have been shown in Figure 9. Silk protein exists in three conformations, namely, random coil, silk I (R form) and silk II (β -sheet) (Warwicker et al., 1954). The absorption bands at 1657, 1525, 1245 and 651 cm^{-1} which correspond to amide I, II, III and V bands, respectively, confirms that the degummed silk fiber was mainly in β -sheet conformation similar to the native silk fibre (Mandal and Kundu, 2008a, b). The corresponding peaks of silk fibroin lyophilized hydrogel were found to be 1625, 1509, 1245 and 667 cm^{-1} respectively indicating the β -sheet conformation at the end of processing through regeneration, gelation and lyophilization. Besides, few more peaks were found in lyophilized fibroin powder at frequencies corresponding to 1327 to 1393 cm^{-1} indicating stretched C-O bonding and the relatively unstable state. All the peaks observed in the three amide band regions varied in their width and intensities.

Thermal analysis

B. mori degummed silk and lyophilized fibroin hydrogel showed different thermogravimetric curves as in Figure 10. As shown in thermogravimetric (TG) curves, the initial weight loss below 100°C was due to the water evaporation (Um et al., 2001). At temperature above 200°C, the weight loss occurred again. However, the silk did not completely decompose even at 700°C. The result

shows that silk fibre underwent of at least three thermal decomposition stages, which are 200 to 300°C, 300 to 350°C and 350 to 400°C. A similar decomposition pattern is observed with lyophilized hydrogel. However the rate of degradation is comparatively faster in this case. The decomposition at approximately 300°C is attributed to a disintegration of the intermolecular side chains during the crystalline melting process, while that at around 400°C is attributed to a main chain disintegration, coupled with simultaneous carbon atom rearrangements (Hirabayashi et al., 1974). It was reported that the decomposition at 300°C indicated the low crystallinity of the unoriented β -type configuration and, therefore it can be said that there is less possibility of obtaining a crystalline β -structure, which occurs in the temperature range of 325 to 330°C. It was found that the weight losses at 400°C were low for the gels due to low water content. This suggests that the fibroin molecules come into close contact with each other during the lyophilization process and form a dense aggregate which could mechanically resist carbon atom rearrangements, thus resulting in low weight losses. This phenomenon of the fibroin molecules could be a possible reason for the lyophilized fibroin gel.

Thermal analysis of degummed silk fibroin and lyophilized fibroin hydrogel has been shown as different thermal calorimetric curve (Figure 11). In the DSC curve of degummed silk of *B. mori*, an endothermic peak starts at 56.8°C and has the maximum at 76.3°C without any trace of exothermic transition due to β -sheet structure of degummed fibroin sample whereas the DSC curve for

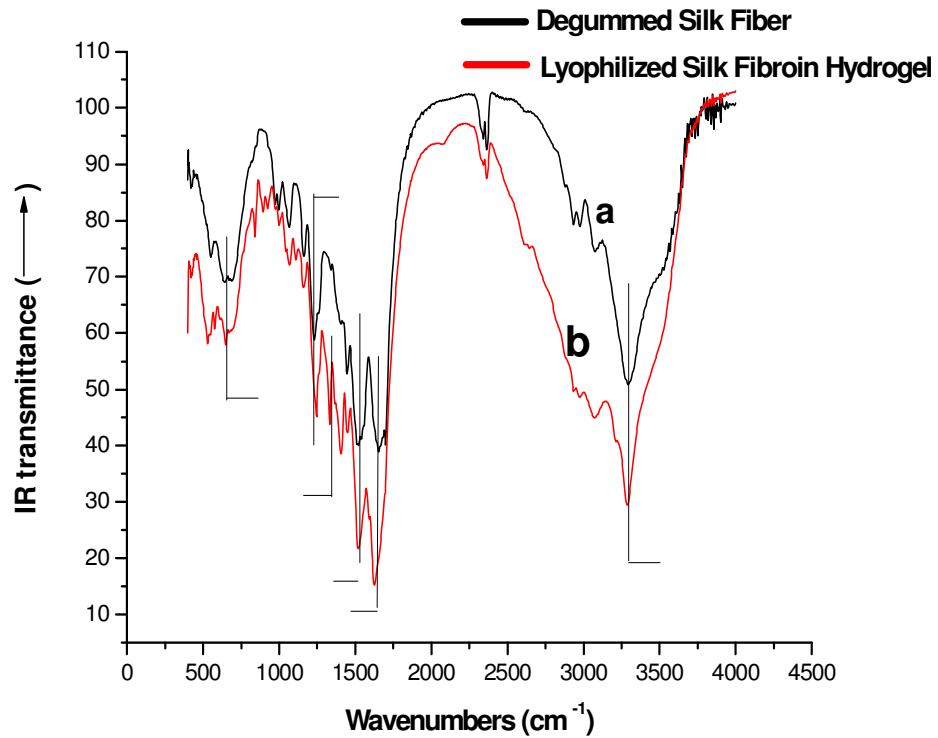


Figure 9. FT-IR spectra of degummed silk fibers (a) and lyophilized silk fibroin hydrogel (b).

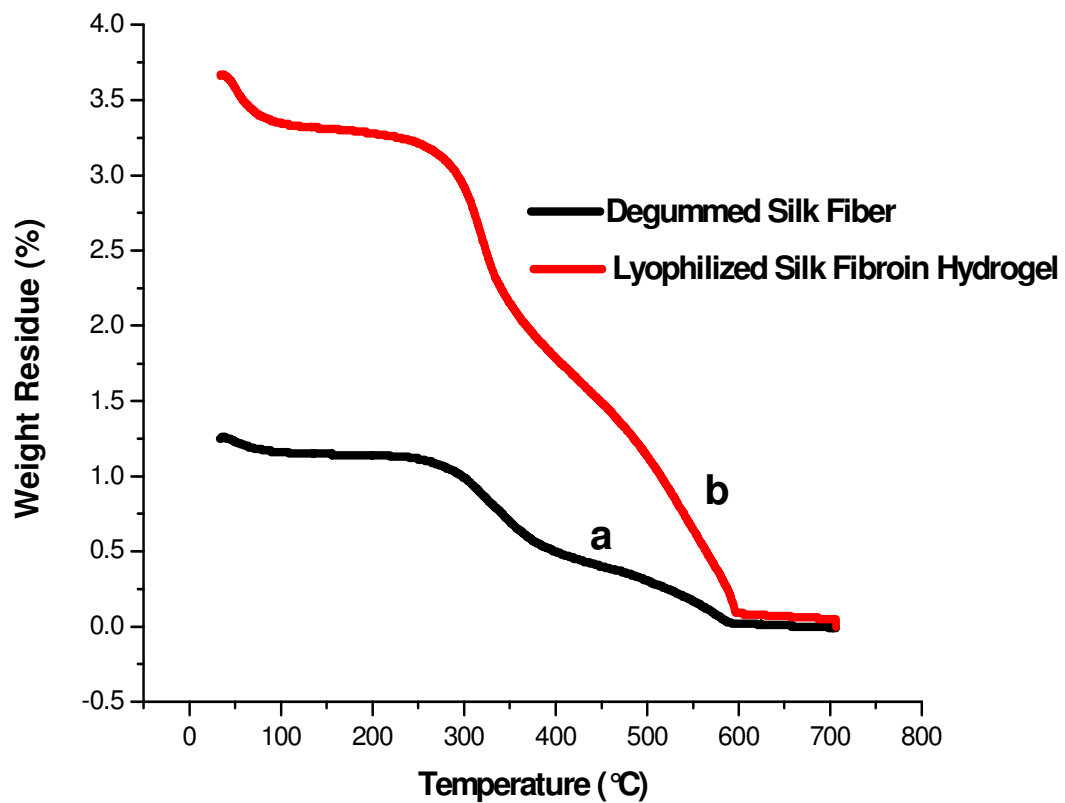


Figure 10. Thermogravimetric(TGA) curves of degummed silk fibers (a) and lyophilized silk fibroin hydrogel (b).

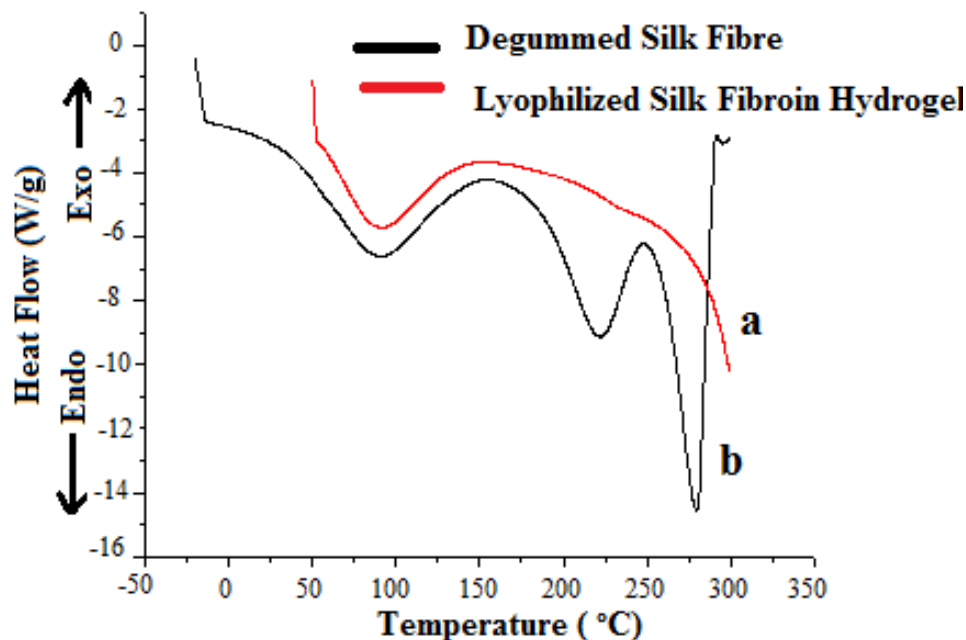


Figure 11. DSC heating curves of degummed *B. mori* silk fibre (a) and lyophilized silk fibroin hydrogel (b).

lyophilized fibroin hydrogel starts at 35.4°C and is maximum at 67.7°C. This difference in results is due to change in β -sheet conformation. A conformational change through the crystallization of SF from random coil to β -sheet causes an exothermic curve to exist. In the DSC curves of two exothermic peaks were observed at around 166 and 255°C which are attributed to conformational change to β -form while two endothermic peaks observed near 220 and 286°C is attributed to the conformational change of β -form into random coils. The exothermic at 220°C indicates the crystallization of the fibroin random coils to α -form of crystals. The decomposition peaks of all the regenerated fibroin materials (endotherms around 290°C) were shifted down compared with the original silk fiber (Warwicker, 1954), indicating the lower thermal stability of regenerated samples. The low thermal stability may be due to lower crystallinity as well as molecular weight decrease during the degumming process of the regenerated fibroin materials compared with the original silk fiber.

hMNC Adherence and proliferation in fibroin hydrogel

hMNCs have been successfully encapsulated in various hydrogel systems due to the potential regeneration of damaged tissue and prolonged drug release. In this study, we isolated hMNCs for the study of cytocompatibility of silk fibroin hydrogels. Due to physical limitation of silk hydrogel of fibroin concentration less than 4% (w/v), the hMNCs were encapsulated in hydrogel system of fibroin concentration more than 4% (w/v). The success

of tissue engineering biomaterials doesn't only rely on the non-toxic and supportive nature to cell adhesion but also on promoting cell proliferation. The photographs in Figure 12 were taken of cells proliferating on hydrogel on consecutive days. Figure 13 shows the adhered mononuclear cells over fibroin hydrogel. Detachment of cells from the substratum was minimal after 2 days *in vitro* cultivation. The morphology of monocytes during *in vitro* cultivation was observed by phase-contrast microscopy. The cells were found to retain round shape and homogenous distribution at day 1 (Figure 12a and b). At day 3, the cells retained their original round shape (Figure 12c). Initially, the monocytes are small (7 to 9 μ m) (Birmingham and Jeska, 1980) and rounded with cytoplasmic spreading. For the 4% gel, hMNCs retained round shape morphology and were nonaggregated in the gel as compared to floating cell clusters in day 1 (Figure 12a) Bar = 100 μ m in all images. The viable cells can be seen as bubbles rounded with trypan stain indicated by arrows.

A progressive enlargement of monocytes occurs in culture with increasing granulation and vascularization of the cytoplasm. After 1 week of cultivation, the monocytes were approximately twice the size of freshly isolated monocytes (Figure 12d). For the 4% gel, cell numbers stopped increasing after 7 days, indicating that maximal gel capacity for cell proliferation was reached. Similar observations were found with hydrogel systems such as alginate and PEG (Figure 14) (Ramdi et al., 1993; Nuttelman et al., 2006). Empty cavities are clearly visible indicating non-supportive behavior towards cell proliferation. hMNCs in more than 4% gels, however, largely

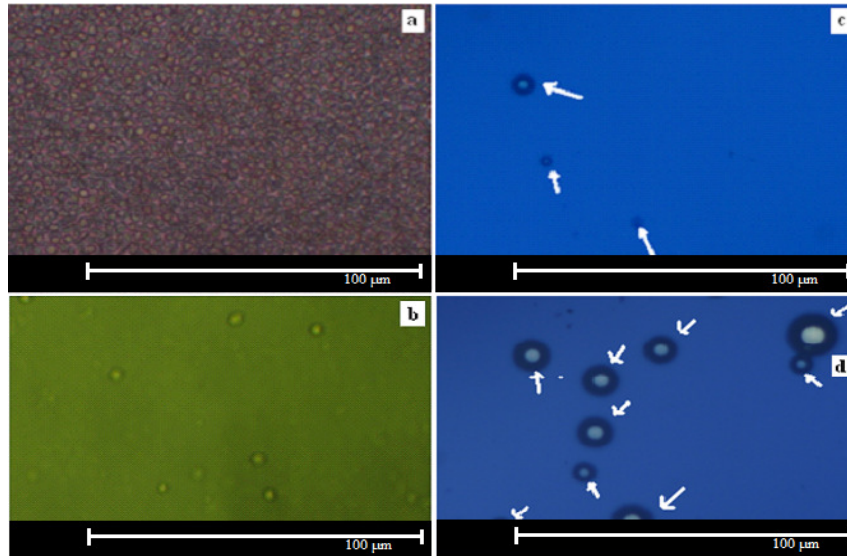


Figure 12. Microscopic imaging of hMNCs encapsulated and cultured in silk fibroin hydrogels at 4% (w/v). Microscopic images were taken at day 1 (a, b), 3 (c) and 7 (d).

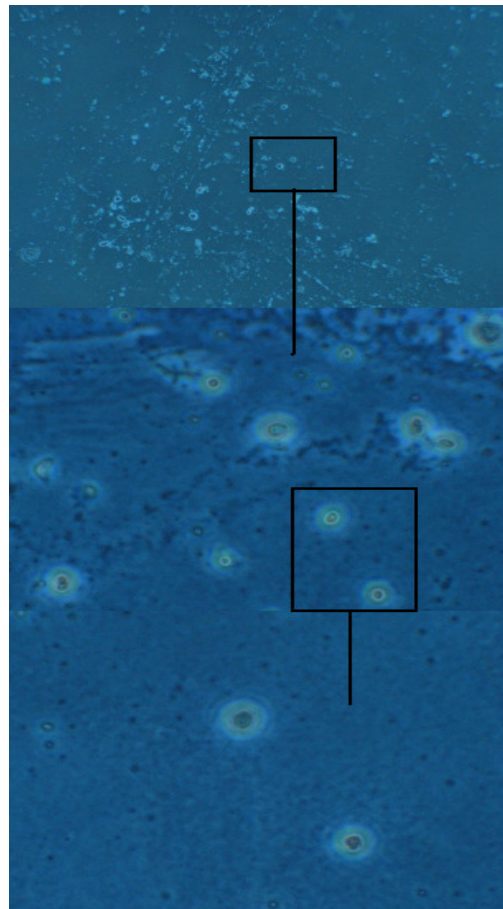


Figure 13. The optical micrographs of hMNCs adhered on the hydrogel surface observed by phase contrast microscope at different magnification. (5X, 10X and 20X).

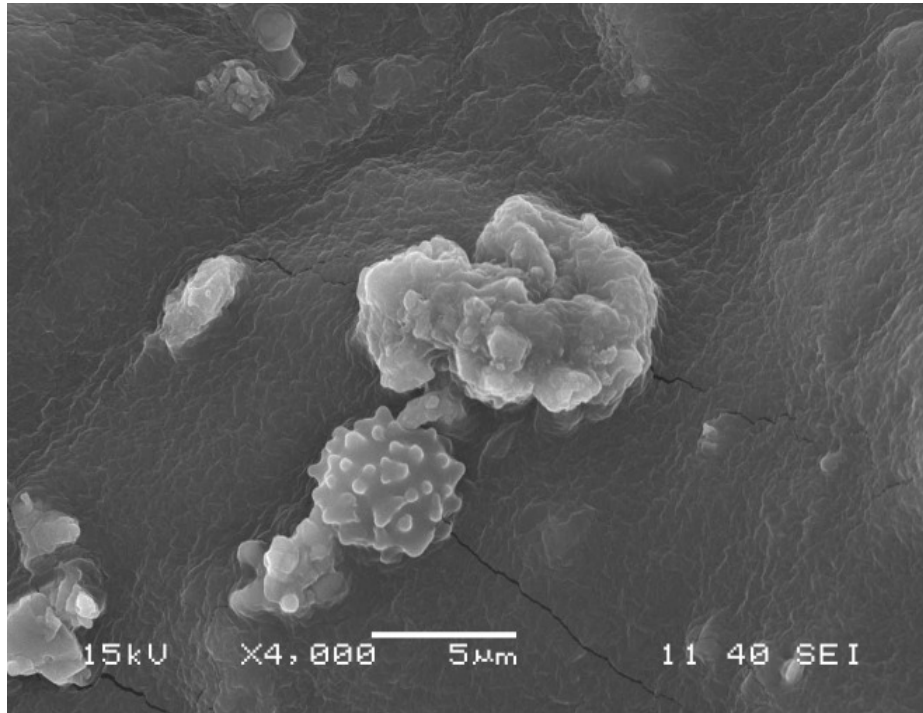


Figure 14. SEM Morphology of cell encapsulated fibroin hydrogel.

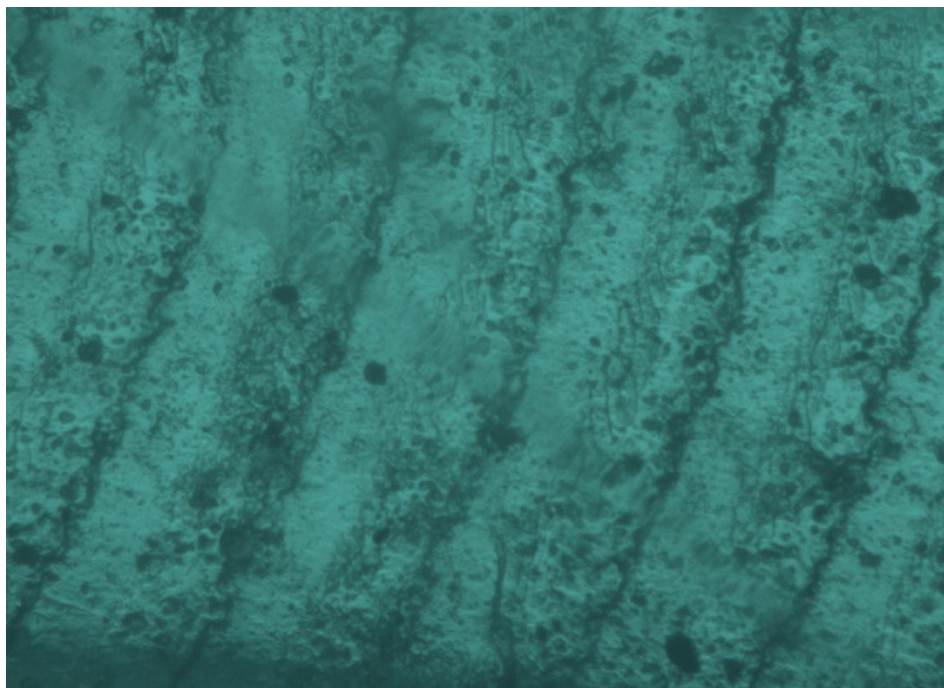


Figure 15. Micrograph of hMNCs seeded fibroin hydrogel with more than 4% concentration cultured over 2 weeks.

changed morphology and many of them died, aggregated and/or dissolved, as seen by the empty cavities in histological images (Figure 15). The loss of activity in the

higher concentration gels is likely due to mechanical restrictions and mass transport limitations. In future studies, the statistical evaluation of fibroin hydrogel *in*

vitro with bone marrow derived mesenchymal stem cells will be entertained.

Conclusions

The main aim of the present study was the preparation, characterization and biorelevant study of silk fibroin hydrogel w.r.t.(with respect to) tissue engineering. Degumming of silk fiber was better at more than 0.02 M Na₂CO₃ at the optimized temperature and time. SEM clearly depicts the complete removal of sericine over the surface. Gel electrophoresis indicated a decreasing amount of the silk 25 kDa light chain and a shift in the molecular weight of the heavy chain. The particle size distribution curve confirmed the result by showing binodal curves around 100 nm and 5 μm. A high strength and a high thermal stability to the dehydrated fibroin gels were obtained by close contact of fibroin molecules. Thermal transition in aqueous solution is a green method in order to obtain a gel with a required volume and shape without incorporating toxic chemicals or other gel inducing solvents. The gel, once formed, has a β-oriented network structure, as a result of intermolecular hydrogen bonding between the molecular components. This stabilizes the confirmation with an additional rotational stability, thus holding the water molecules in the said structure. Rheological and swelling behaviors of fibroin hydrogel were appreciable at 37°C to mimic the body tissue. Results from study of secondary structure and crystallinity favor the stability and strength of lyophilized hydrogen as supportive biomaterial. Thermal analysis support that silk as biomaterial with predictable long-term degradation characteristics.

The cytocompatibility of fibroin hydrogel against hMNCs were found positive. hMNCs adherence, growth and proliferation indicates their good interface effect. Well interconnected and open pores in three-dimensional network provided optimal microenvironment for cell's adherence, proliferation and growth acting as framework for newly-formed tissues. The regenerated fibroin solution can also be used for thin films or 3D scaffold fabrication. An improved understanding of the *in vivo* environment and their role in the degradation of silk fibroin will provide the next logical step in modeling an appropriate long-term degradable scaffold for various tissue engineering applications.

ACKNOWLEDGEMENTS

The authors would like to thank Mr. Rajesh Patnayak, Lab Technician in Department of Metallurgy and Material Science, NIT Rourkela for FTIR study and Mr. Sarad Kumar, Research Scholar in Department of Ceramic Engineering, NIT Rourkela for XRD Analysis. They would like to thank the unknown reviewers for their valuable

comments to improve the quality of the manuscript.

REFERENCES

- Altman GH, Diaz F, Jakuba C, Calabro T, Horan RL, Chen J, Lu H, Richmond J, Kaplan DL (2003). Silk based biomaterials. *Biomaterials*, 24: 401-416.
- Asakura T, Kuzuhara A, Tabeta R, Saito H (1985). Conformational characterization of B. mori silk fibroin in the solid state by high-frequency 13 C cross polarization-magic angle spinning NMR, X-ray diffraction and infrared spectroscopy. *Macromolecules*, 18: 1841-1845.
- Ayub ZH, Arai M, Hirabayashi K (1993). Mechanism of the gelation of fibroin solution. *Biosci. Biotechnol. Biochem.*, 57: 1910-1912.
- Ayub ZH, Arai M, Hirabayashi K (1994). Quantitative structural analysis and physical-properties of silk fibroin hydrogels. *Polymer*, 35: 2197-2200.
- Balakrishnan B, Jayakrishnan A (2005). Self-cross-linking biopolymers as injectable in situ forming biodegradable scaffolds. *Biomaterials*, 26(18): 3941-3951.
- Birmingham JR, Jeska EL (1980). The isolation, long-term cultivation and characterization of bovine peripheral blood monocytes. *Immunology*, 41: 807.
- Drury JL, Mooney DJ (2003). Hydrogels for tissue engineering: scaffold design variables and applications. *Biomaterials*, 24: 4337-4351.
- Fini M, Motta A, Torricelli P, Giavaresi G, Aldini NN, Tschon M, Giardino R, Migliaresi C (2005). The healing of confined critical size cancellous defects in the presence of silk fibroin hydrogel. *Biomaterials*, 26(17): 3527-3536.
- Hanawa T, Watanabe A, Tsuchiya T, Ikoma R, Hidaka M, Sugihara M (1995). New Oral dosage form for elderly patients: Preparation and characterization of silk fibroin gel. *Chem. Pharm. Bull.*, 43: 284-288.
- Hirabayashi K, Sujuki T, Nagyra M, Ishikawa H (1974). Thermal analysis of sericin cocoon. *Bunseki kiki*, 12: p. 437.
- Hofmann S, Wong CT, Foo P, Rossett F, Textor M, Vunjak-Novakovic G, Kaplan DL, Merklea HP, Meinel L (2006). Silk fibroin as an organic polymer for controlled drug delivery. *J. Control Release*, 111: 219-227.
- Horan RL, Antle K, Collette AL, Wang Y, Huang J, Moreau JE, Volloch V, Kaplan DL, Altman GH (2005). *In vitro* degradation of silk fibroin. *Biomaterials*, 26(17): 3385-3393.
- Kang GD, Nahm JH, Park JS, Moon JY, Cho CS, Ye JH (2000). Effects of poloxamer on the gelation of silk fibroin. *Macromol. Rapid Commun.*, 21: 788-791.
- Kang GD, Nahm JH, Park JS, Moon JY, Cho CS, Yeo JH (2000). Effects of poloxamer on the gelation of silk fibroin. *Macromol. Rapid Commun.*, 21: 788-791.
- Kaplan DL, Adams WW, Farmer B, Viney C (1994). Silk-biology, structure, properties, and genetics. *ACS Symp. Ser.*, 544: 2-16.
- Kim UJ, Park J, Li C, Jin HJ, Valluzzi R, Kaplan DL (2004). Structure and properties of silk hydrogels. *Biomacromolecules*, 5: 786-792.
- Kretlow JD, Klouda L, Mikos AG (2007). Injectable matrices and scaffolds for drug delivery in tissue engineering. *Adv. Drug Deliv. Rev.*, 59(4-5): 236-273.
- Laemmli UK (1970). Cleavage of structural proteins during the assembly of the head of bacteriophage T4. *Nature*, 227(259): 680-685.
- Lee CH, Singla A, Lee Y (2001). Biomedical applications of collagen. *Int. J. Pharm.*, 221: 1-22.
- Lee KY, Mooney DJ (2001). Hydrogel for tissue engineering. *Chem. Rev.*, 101: 1869-1879.
- Li C, Vepari C, Jin HJ, Kim HJ, Kaplan DL (2006). Electrospun silk-BMP-2 scaffolds for bone tissue engineering. *Biomaterials*, 27: 3115-3124.
- Li M, Lu S, Wu Z, Yan H, Mo J, Wang LJ (2001). Study on porous silk fibroin materials. I. Fine structure of freeze dried silk fibroin. *Appl. Polym. Sci.*, 79: 2185-2191.
- Magoshi J, Magoshi Y, Becker MA, Nakamura S (1996). Biospinning (Silk fibre formation, multiple spinning mechanism), in *Polymeric Materials Encyclopedia* (Ed. Salamone JC) CRC Press, Boca Raton

- (FL, USA), 1: 667-679.
- Mandal BB, Kundu SC (2008a). Non-bioengineered silk fibroin protein 3D scaffolds for potential biotechnological and tissue engineering applications. *Macromol. Biosci.*, 8: 807-818.
- Mandal BB, Kundu SC (2008b). Non-bioengineered silk gland fibroin protein: characterization and evaluation of matrices for potential tissue engineering applications. *Biotechnol. Bioeng.*, 100: 1237-1250.
- Miller JT (1960). *The Instrument Manual 3rd Ed.* United Trade Press Ltd.. London.
- Motta A, Miglilaresi C, Faccioni F, Torricelli P, Fini M, Giardino R (2004). Fibroin hydrogels for biomedical applications: preparation, characterization and in vitro cell culture studies. *J. Biomater. Sci. Polymer Ed.*, 15: 851-864.
- Neagu M, Suci E, Ordodi V, Paunescu V (2005). Human mesenchymal stem cells as basic tools for tissue engineering: Isolation and Culture. *Romanian J. Biophys.*, 15 (1-4): 29-34.
- Nuttelman CR, Benoit DS, Tripodi MC, Anseth KS (2006). The effect of ethylene glycol methacrylate phosphate in PEG hydrogels on mineralization and viability of encapsulated hMSCs. *Biomaterials*, 27: 1377-1386.
- Ochi A, Hossain KS, Magoshi J, Nemoto N (2002). Rheology and Dynamic Light Scattering of Silk Fibroin Solution Extracted from the Middle Division of *Bombyx mori* Silkworm. *Biomacromolecules*, 3(6): 1187-1196.
- Park JB, Lakes RS (1992). *Biomaterials: an introduction*. Vol. 2. Plenum Press. New York.
- Peppas NA (1997). A practical approach to body building. *Nature (London)*, 389: 453.
- Ramdi H, Legay C, Lievreumont M (1993). Influence of matricial molecules on growth and differentiation of entrapped chondrocytes. *Exp. Cell Res.*, 207: 449-454.
- Smart JD (2005). The basics and underlying mechanisms of mucoadhesion. *Adv. Drug Deliv. Rev.*, 57: 1556-1568.
- Smart JD, Kellaway IW, Worthington HEC (1984). An *in vitro* investigation of mucosa –adhesive materials for use in controlled drug delivery. *J. Pharm. Pharmacol.*, 36: 295-299.
- Smidsrod O, Skjaok-Br k G (1990). Alginate as immobilization matrix for cells. *Trends Biotechnol.*, 8: 71-78.
- Uebersax L, Merkle HP, Meinel L (2008). Insulin-like growth factor I releasing silk fibroin scaffolds induce chondrogenic differentiation of human mesenchymal stem cells. *J. Control Release*, 127: 12-21.
- Um IC, Kweon HY, Park YH, Hudson S (2001). Structural characteristics and properties of the regenerated silk fibroin prepared from formic acid. *Int. J. Biol. Macromol.*, 29: 91-97.
- Vazquez B, Roman JS, Peniche C, Cohen ME (1997). Polymeric hydrophilic hydrogels with flexible hydrophobic chains control of the hydration and interaction with water molecules. *Macromolecules*, 30: 8440-8446.
- Vepari C, Kaplan DL (2007). Silk as a biomaterials. *Prog. Polym. Sci.*, 32: 991-1007.
- Wang X, Wenk E, Matsumoto A, Meinel L, Li C, Kaplan DL (2007). Silk microspheres for encapsulation and controlled release. *J. Control Release*, 117: 360-370.
- Warwicker JO (1954). The crystal structure of silk fibroin. *Acta Cryst.*, 7: 565-573.